Low loss Nb_2O_5 films deposited by novel remote plasma sputtering*

LIU Zhe (刘哲) **and BU Yi-kun** (卜轶坤)**
Department of Electronic Engineering, Xiamen University, Xiamen 361005, China

(Received 25 November 2012)
©Tianjin University of Technology and Springer-Verlag Berlin Heidelberg 2013

We report the deposition of Nb_2O_5 films on unheated BK-7 glass substrates using remote plasma sputtering system. The remote plasma geometry allows pseudo separation of plasma and target bias parameters, which offers complete deposition rate control. Using appropriate oxygen flow rates, high-density and low-loss Nb_2O_5 films are deposited with rates up to 0.49 nm/s. Lower deposition rates (~0.026 nm/s) can also be obtained by working at low target current and voltage and at low pressure. Nb_2O_5 films deposited at different rates have the refractive index of about 2.3 and the extinction coefficient as low as 6.9×10^{-5}.
Document code: A **Article ID:** 1673-1905(2013)02-0116-4
DOI 10.1007/s11801-013-2406-y

Niobium oxide films are increasingly applied in various fields[1-4]. Niobium pentoxide (Nb_2O_5) films have been prepared by different deposition processes[5-9]. However, conventional magnetron sputtering deposition (MSD) is limited by low target utilization, deposition rate, uniformity and ion bombardment of the target. Formation of the race-track and target poisoning usually leads to plasma instability and shift of deposition rate, and thus feedback control is often required to keep the process stable[10-12]. High quality Nb_2O_5 films can be obtained by ion-beam sputtering deposition (IBSD), too. However, to get low loss Nb_2O_5 films, the deposition rate of IBSD has to be reduced to a very slow value (< 0.06 nm/s), and parts of the coatings need to be post-baked for several hours[13].

To overcome the disadvantages of conventional MSD as well as keep a high deposition rate, remote plasma sputtering deposition (RPSD) is demonstrated[14]. It provides a high-density plasma and low-energy ion bombardment (~10 eV) at the substrate. Due to the removal of the magnetron at the back side of the target, the sputtering erosion occurs across the full surface of the target, leading to more than 90% target utilization. This feature avoids the race-track formation on the target surface inherent with magnetron sputtering, and results in significant reduction in target poisoning[15]. S. J. Wakeham et al[16] studied the properties of indium tin oxide (ITO) films prepared using this sputtering technology. In this paper, low-loss Nb_2O_5 films are prepared by using remote plasma sputtering deposition system. The pseudo-independence of target current and voltage in the deposition system offers complete deposition rate control. Wide deposition rate range from 0.49 nm/s to 0.026 nm/s is achieved.

The general description of the remote plasma sputtering system has been reported previously[16]. A schematic diagram of the system is shown in Fig.1. The coating process utilizes a remote, high-density (of the order of 10^{13} ions/cm^3) argon plasma which is generated in a side arm adjacent to the deposition chamber. Briefly, the plasma is generated by a 13.56 MHz radio frequency (RF) source, focused by a launch electromagnet, and directed towards the target using a second electromagnet. The substrate holder is placed opposite the target. Mass flow controllers regulate the flow of argon and oxygen gases into the chamber via distribution rings located at the target and substrate, respectively. With the application of a negative direct current (DC) bias to the target, the argon ions are accelerated across the target sheath. This yields high rate and uniform erosion of the target surface. Inset of Fig.1 shows the niobium target which has been uniformly eroded. The distance between the target and substrate is 26 cm.

The remote plasma geometry is physically composed of the plasma generation region and the target bias region, which makes the deposition system allow for independent setting of the target voltage (DC power supply) and target current (RF power supplied to the plasma). As the target is not required to strike or maintain the plasma, the remote plasma generation in the sputtering system offers a solution to the power constraints of conventional magnetron sputtering. Fig.2 shows the target current as a function of target voltage for four values of the remote plasma source RF power.

* This work has been supported by the Natural Science Foundation of Fujian Province of China (No. 2010J01349).
** E-mail: buyikun139@163.com

The target current saturates above approximately 100 V, and there exists a pseudo-independence of target current and voltage. The pseudo-independence of target current and voltage offers a great deal of flexibility with regard to the control of growth conditions and film properties.

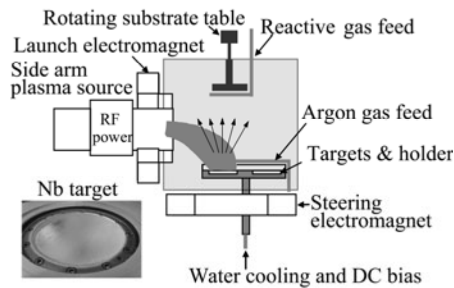

Fig.1 Schematic diagram of the remote plasma sputtering system (Inset shows the niobium target which has been uniformly eroded.)

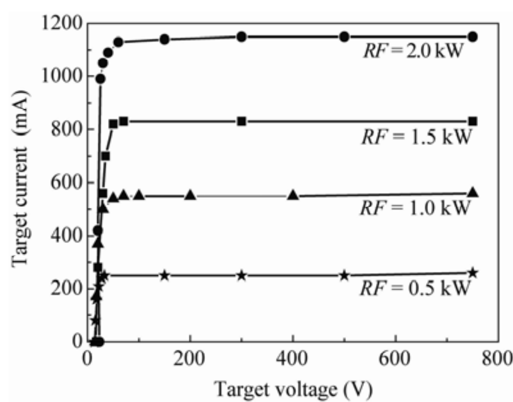

Fig.2 Dependence of the sputtering target current on the target voltage and remote plasma source RF power at an argon pressure of 0.4 Pa

Nb_2O_5 films were deposited on unheated BK-7 glass by reactively sputtering from a niobium target with purity of 99.99%, diameter of 102 mm and water cooled. The glass substrates were sequentially cleaned in an ultrasonic bath with acetone and ethanol. For each deposition, the base pressure was at most 5.3×10^{-4} Pa. All the substrates underwent preconditioning in diffuse, low intensity plasma prior to the deposition. The substrates were not biased for this stage of the process, and the impinging low energy argon ions were seen to remove volatile species from the surface of the substrate, resulting in excellent film adhesion. Then the target surface was cleaned by sputtering in a pure argon atmosphere in order to remove oxide layers.

To get a high rate deposition, the RF power source was set to 2 kW, and the target was biased to 700 V. Argon gas flow was fixed at 70 cm^3/min, while oxygen flow was varied from 0 to 30 cm^3/min. Fig.3 shows the deposition rate measured by a telemark model 880 quartz crystal thickness monitor. The deposition rate initially increases and then decreases with increasing oxygen flow rate.

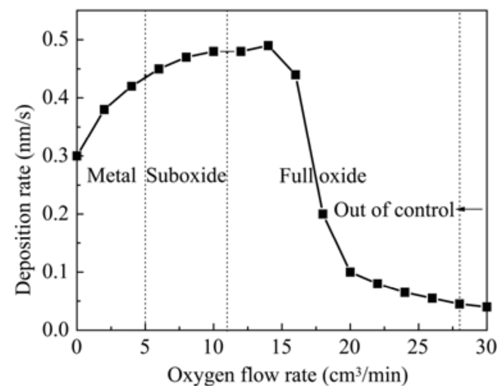

Fig.3 Deposition rate as a function of oxygen flow rate

This effect is attributed primarily to the transition of the sputtering between three modes as the metal mode, the suboxide mode and the full oxide mode. At an oxygen flow rate below 5 cm^3/min, Nb atoms were deposited, indicating that the amount of oxygen is too little to react with the Nb atoms to form an oxide layer on the substrate. As the reactive gas flow increased, more and more oxygen gas reacted with the sputtered Nb atoms, showing a rising up deposition rate. However, the oxygen gas was still insufficient to get a perfect stoichiometry, hence niobium suboxide was formed. When the oxygen flow rate reached 12 cm^3/min, the Nb atoms were completely oxidized, and stable oxide film (Nb_2O_5) was formed. The deposition rate reached 0.49 nm/s when the oxygen flow rate increased to 14 cm^3/min. When the oxygen flow rate was set to more than 14 cm^3/min, the deposition rate dropped precipitously, because the target compound coverage increased, and there was less sputtered target material to combine with the reactive gas. When the target surface was almost covered with the compound material, the deposition rate remained stable, and the Nb atoms were still completely oxidized. The reduction of deposition rate is the property for many elements reactively sputtered in Ar/O_2 mixtures when the transition from the metal mode to the oxide mode occurs. However, after an insulating film formed on the target surface, electric arc may occur. Although it could be avoided by pulsed DC power at a certain extent, too much oxygen (equal or more than 28 cm^3/min) leaded to out of control of the sputtering process.

As well as high rate deposition of Nb_2O_5 films, the system can be used for low rate work. To get a low rate deposition, we used target voltage and remote plasma RF power as the primary process control parameters, and oxygen gas flow as the secondary process parameter. A lower deposition rate of 0.026 nm/s was obtained with a target power density of 0.36 W/cm^2.

Fig.4 presents the transmittance spectra of Nb_2O_5 films deposited by remote plasma sputtering with oxygen flow rates of 4 cm^3/min, 8 cm^3/min, 12 cm^3/min and 16 cm^3/min. The RF power source was set to 2 kW, and the target was biased to 700 V, while the argon gas flow was fixed at 70 cm^3/min. Transmittance measurements were performed by a Perkin-Elmer Lambda 750 spectrometer. The transmittance of bare glass was measured as a reference, too. According to the spectra, some niobium metals were deposited at a flow rate of 4 cm^3/min, and they can strongly absorb visible light. At a flow rate of 8 cm^3/min, niobium suboxides were formed. The transmittance increased a lot, while absorption was still obvious. The threshold flow rate of oxygen gas was about 12 cm^3/min. A flow rate above 12 cm^3/min provided sufficient oxygen molecules to react with the Nb atoms on the substrate.

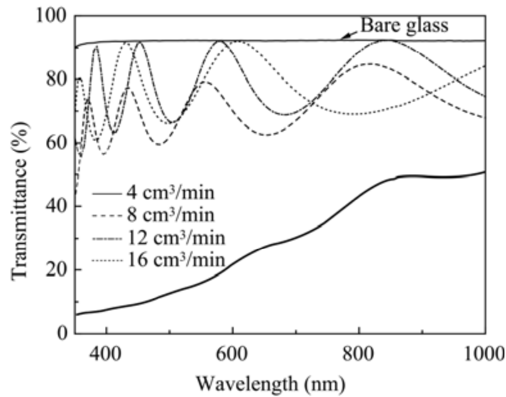

Fig.4 Transmittance spectra of Nb_2O_5 films prepared at different oxygen flow rates

From the spectral analysis, the refractive index n, the extinction coefficient k and the physical thickness d of the films are determined by the envelop method[17]. Based on the above measurement, the refractive index and extinction coefficient at a wavelength of 650 nm with increasing oxygen flow rate in the full oxide window are calculated and plotted in Fig.5. The refractive index does not change too much, while the extinction coefficient is dependent on the oxygen flow rate. The extinction coefficient value is decreased from 4.5×10^{-4} to 6.9×10^{-5} as the oxygen flow rate varies from 12 cm^3/min to 24 cm^3/min. The lowest extinction coefficient is obtained at a flow rate of 16 cm^3/min. The extinction coefficient increases a little when the oxygen flow rate increases from 16 cm^3/min to 24 cm^3/min, possibly because the unneeded gas was trapped in the film and made voids in it, and thus the scattering increased. Comparison of deposition rates and optical properties of Nb_2O_5 films deposited by different sputtering technologies can be seen from Tab.1. Compared with those deposited by IBSD and conventional MSD, the Nb_2O_5 films deposited by RPSD bear great potential to be high refractive material for optical interference filters due to their low extinction coefficient and wide control range of deposition rate.

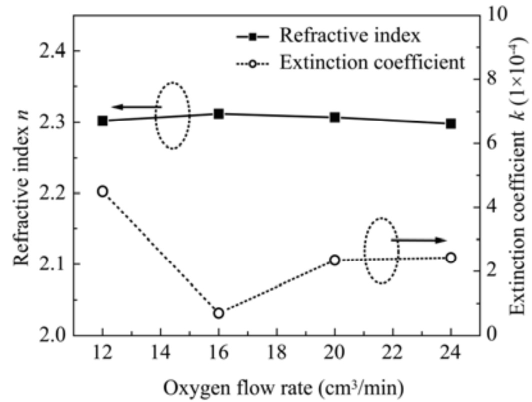

Fig.5 Refractive index and extinction coefficient at wavelength of 650 nm as a function of oxygen flow rate

Tab.1 Comparison of deposition rates and optical properties of Nb_2O_5 films deposited by different sputtering technologies

Method	IBSD	IBSD	MSD	MSD	RPSD
Deposition rate (nm/s)	0.06−0.09	0.05−0.12	0.56−1.66	-	0.03−0.49
Calculated wavelength (nm)	633	633	500	650	650
Refractive index	~2.3	2.3	2.1−2.3	2.2−2.3	~2.3
Extinction coefficient (10^{-4})	3	2−6	<50	~3	0.69−4.5
Need post-baking	Yes	Yes	No	No	No
Reference	[8]	[13]	[9]	[6]	This paper

In conclusion, a process is presented to prepare low loss Nb_2O_5 films by using remote high density plasma. Deposition rate can be controlled flexibly from 0.026 nm/s to 0.49 nm/s because of the pseudo-independence of target current and voltage. For higher rate, different deposition rates are obtained by keeping the RF power and target bias at a high level and meanwhile changing the oxygen flow rate. The lower deposition rate can be obtained by working at a low target current and voltage and at low pressure. The refractive index can keep stable (~2.3), while the extinction coefficient varies from 4.5×10^{-4} to 6.9×10^{-5} at different oxygen flow rates.

References

[1] T. Maruyama and S. Arai, Appl. Phys. Lett. **63**, 869 (1993).
[2] M. T. Duffy, C. C. Wang, A. Waxman and K. H. Zaininger, J. Electrochem. Soc. **116**, 234 (1969).
[3] G. Korotcenkov, Mater. Sci. Eng. B **139**, 1 (2007).
[4] Y. Saito and T. Shiosaki, Jpn. J. Appl. Phys. **31**, 3164 (1992).
[5] J. J Van Glabbeek and R. E Van De Leest, Thin Solid

Films **201**, 137 (1991).

[6] F. Lai, L. Lin, Z. Huang, R. Gai and Y. Qu, Appl. Surf. Sci. **253**, 1801 (2006).

[7] S. Venkataraj, D. Severin, S. H. Mohamed, J. Ngaruiya, O. Kappertz and M. Wuttig, Thin Solid Films **502**, 228 (2006).

[8] C. C. Lee, J. C. Hsu and D. H. Wong, Appl. Surf. Sci. **171**, 151 (2001).

[9] S. Venkataraj, R. Drese, O. Kappertz, R. Jayavel and M. Wuttig, Phys. Stat. Sol. A **188**, 1047 (2001).

[10] W. D. Sproul, D. J. Christie and D. C. Carter, Thin Solid Films **491**, 1 (2005).

[11] F. Wang, X. L. Chen, X. H. Geng, Q. Huang, D. K. Zhang, J. Sun, C. C. Wei, X. D. Zhang and Y. Zhang, Journal of Optoelectronics • Laser **23**, 724 (2012). (in Chinese)

[12] H. F. Liu, C. X. Lei and H. F. Zhang, Journal of Optoelectronics • Laser **23**, 730 (2012). (in Chinese)

[13] C. C. Lee, J. C. Hsu, D. T. Wei and D. H. Wong, Opt. Quantum Electron. **32**, 327 (2000).

[14] M. Vopsaroiu, M. J. Thwaites, S. Rand, P. J. Grundy and K. O'Grady, IEEE Trans. Magn. **40**, 2443 (2004).

[15] G. Claudio, S. Calnan, K. Bass and M. Boreland, J. Mater. Sci. Mater. Electron. **19**, S285 (2008).

[16] S. J. Wakeham, M. J. Thwaites, B. W. Holton, C. Tsakonas, W. M. Cranton, D. C. Koutsogeorgis and R. Ranson, Thin Solid Films **518**, 1355 (2009).

[17] R. Swanepoel, J. Phys. E: Sci. Instrum. **16**, 1214 (1983).